Migration enthalpies in FCC and BCC metals

1992 J. Phys.: Condens. Matter 4 9321

(http://iopscience.iop.org/0953-8984/4/47/013)

J. Phys.: Condens. Matter 4 (1992) 9321–9338. Printed in the UK

Migration enthalpies in FCC and BCC metals

H R Schober†, W Petry‡ and J Trampenau‡§

† Institut für Festkörperforschung der KFA-Jülich, Postfach 1913, D-5170 Jülich, Federal Republic of Germany

‡ Institut Laue Langevin, 156X, F-38042 Grenoble Cédex, France

§ Institut für Metallforschung, Universität Münster, D-4400 Münster, Federal Republic of Germany

Received 21 April 1992

Abstract. We present a model relating the migration enthalpy H_v^m for nearest-neighbour vacancy jumps in cubic metals to the phonon dispersion. The migration enthalpy is split into two parts, one depending only on the lattice structure, the other on the vibrational properties of the particular metal. This latter term can be written in terms of the static lattice Green function, i.e. of the ω^{-2} moment of the spectrum. It can thus be calculated directly from measured phonon dispersion curves. For FCC metals, excellent agreement between calculated and measured values of H_v^m is found. For BCC metals, where H_v^m is known from experiments only in a few cases, predictions are made wherever the phonon dispersions are available. The model takes into account the unusually low-lying phonon branches in some of the BCC metals and yields, where phonon frequencies shift with temperature, temperature-dependent values of H_v^m.

1. Introduction

Compared to those of the FCC metals, self-diffusion coefficients $D(T)$ in BCC metals are known for their anomalous behaviour. Comparing $D(T)$ on a temperature scale normalized by the respective melting temperature T_m, the self-diffusion data in BCC metals (figure 1(*a*)) scatter over a large range, whereas those of the FCC metals (figure 1(*b*)) fall within a small band described by the activation energy Q and the prefactor D_0:

$$Q = 1.5 \times 10^{-3} T_m (\pm 10\%) \text{ eV}$$

$$0.05 \leqslant D_0 \leqslant 5 \times 10^{-4} \text{ m}^2 \text{ s}^{-1}.$$

The variation of the diffusivities in BCC metals exhibits some group systematics [1, 2]. Group VI metals, where the BCC structure is the only stable phase and which have high melting temperatures, show the lowest diffusivities. Those of the group V metals, (V, Nb and Ta) are slightly higher and similar to the ones of the FCC metals. The BCC metals with a limited existence range like the alkali metals (Li, K and Na) and even more pronounced the group IV metals (Ti, Zr and Hf) show much higher diffusivities in their BCC phase.

The differences are strongest at low temperatures, whereas diffusivities extrapolated to the melting point approach a common value

$$10^{-12} \leqslant D(T_m) \leqslant 5 \times 10^{-11} \text{ m}^2 \text{ s}^{-1}.$$

0953-8984/92/479321+18$07.50

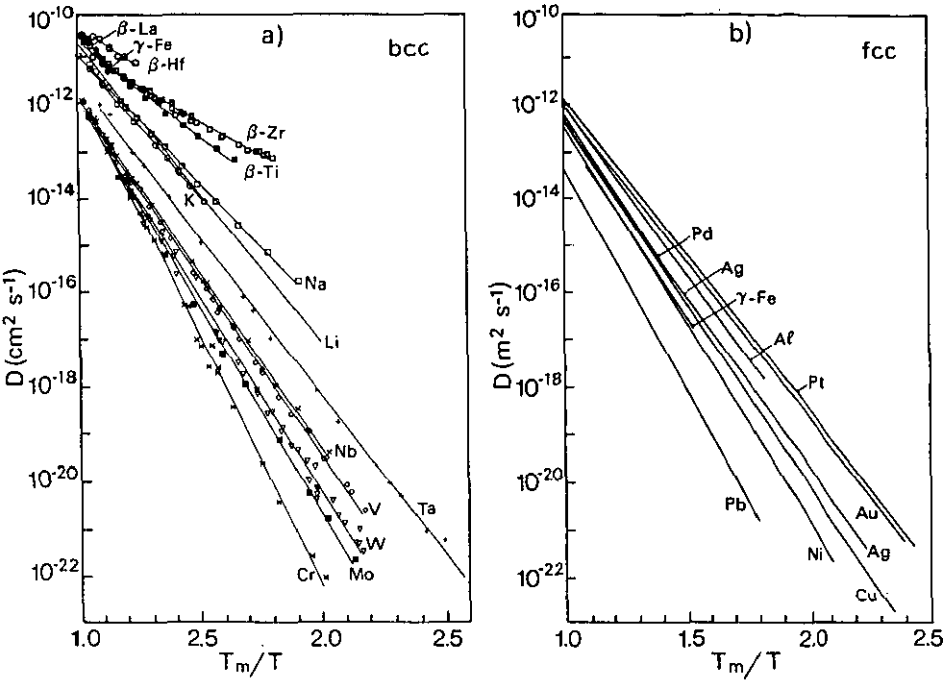

Figure 1. (*a*) Self-diffusivities D of BCC metals on a normalized temperature scale. (*b*) For comparison, the self-diffusivity D of FCC metals on a similar scale. For a compilation of $D(T)$ see [28].

The most pronounced curvatures in the Arrhenius plot of $D(T)$ are observed for the BCC metals with the highest diffusivities. Deviations from a linear behaviour are also reported for the more 'normal' metals Ta, Nb, V, W and Mo [3]. Only the diffusivity of Cr, which is the lowest of all BCC metals, can be described well by a single activation energy over a temperature range $1 \leqslant T_m/T < 2$ [4].

It is commonly accepted that self-diffusion in FCC metals is dominated by the most simple mechanism, namely $\frac{1}{2}\langle 110\rangle$ diffusion jumps into nearest-neighbour (NN) vacancies [5]. Whether the self-diffusivities in all BCC metals can be understood in a similar simple picture, namely in terms of diffusion via $\frac{1}{2}\langle 111\rangle$ NN vacancy jumps, is less evident. Such a model has to explain why the diffusion entropies and enthalpies vary over a large range for the different elements of a common structure. Furthermore, in order to explain the curved Arrhenius plots, it has to introduce temperature dependences of these quantities. In the model proposed by Herzig [2, 6] and Petry [7, 8] this is *qualitatively* achieved by pointing out the striking correlation between phonon and diffusion anomalies in BCC metals. It is argued that the extraordinary low phonon frequencies found in BCC elements probe the migration potential for the diffusion jump into NN vacancies and thus are experimental evidence for low migration barriers. The different degree of softening observed in the different elements then accounts for the large scatter in the heights of the migration barrier. Newly available temperature-dependent phonon measurements in the BCC phase of the group IV metals [9–11] show the predicted pronounced frequency shift of these low-frequency phonons with temperature. This experimental proof of the strong anharmonicity in these metals is the crucial prerequisite to define temperature-

dependent entropies and enthalpies.

Direct experimental evidence for the dominance of the NN vacancy jump mechanism for the self-diffusion in BCC metals was found in recent quasi-elastic neutron scattering experiments on Na [12, 13] and β-Ti [14]. Emphasis is put on the case of β-Ti, which shows the most striking diffusion anomalies and was thought to be an ideal candidate for alternative diffusion mechanisms.

It is the purpose of this paper to calculate the migration enthalpy H_v^m for an NN vacancy jump *directly from the measured phonon dispersion* without adjustable parameters. Comparison with experimentally known values of H_v^m will show the validity of such a model of phonon-controlled diffusion. Reliable predictions can be made for cases where H_v^m is not accessible experimentally, e.g. in metals where the BCC structure is stable only at high temperatures.

The paper is organized as follows. In section 2 the formalism to calculate H_v^m by means of the phonon density of states is presented. In section 3 calculations of H_v^m for FCC metals are compared with the experimentally known values. Encouraged by the success of our model in the case of the FCC metals, H_v^m is calculated in section 4 for BCC metals, where the experimental situation is less clear. In section 5 the temperature dependence of $H_v^m(T)$ is calculated for BCC metals, where phonon dispersions are known in the temperature range relevant to diffusion. Finally in section 6 it is shown that in the two extreme cases—namely fast diffusion and strongly curved Arrhenius plot in β-Zr, and slow diffusion and straight Arrhenius plot in Cr—$D(T)$ can be explained by the same mechanism, diffusion via NN vacancies.

2. The model

2.1. General

For a monovacancy jump in cubic lattices, the self-diffusion constant $D(T)$ can be expressed by

$$D(T) = a^2 f w_v(T) c_v(T) \tag{1}$$

with a the lattice parameter, f the correlation factor ($f_{FCC} = 0.782$, $f_{BCC} = 0.727$), $w_v(T)$ the migration jump probability

$$w_v(T) = n_0 \exp(S_v^m/k_B) \exp(-H_v^m/k_B T) \tag{2}$$

and $c_v(T)$ the probability of finding a vacancy on a given lattice site, i.e. the vacancy concentration

$$c_v(T) = \exp(S_v^f/k_B) \exp(-H_v^f/k_B T). \tag{3}$$

According to the theory of Vineyard [15], the entropies can be expressed by the eigenfrequencies for the equilibrium configuration ω_α^e ($\alpha = 1, \ldots, 3N$) and those of the defect configuration. The latter are the eigenfrequencies of either the saddle-point configuration ω_α^s ($\alpha = 1, \ldots, 3N-1$) or of a lattice containing a vacancy ω_α^v ($\alpha = 1, \ldots, 3N$).

In the high-temperature limit, the migration and the formation entropies are given by

$$S_v^m = k_B \ln\left(\prod_{\alpha=1}^{3N-1} \omega_\alpha^e \Big/ \prod_{\alpha=1}^{3N-1} \omega_\alpha^s \right) \tag{4}$$

$$S_v^f = k_B \ln\left(\prod_{\alpha=1}^{3N} \omega_\alpha^e \Big/ \prod_{\alpha=1}^{3N} \omega_\alpha^v \right). \tag{5}$$

In equation (4) the attempt frequency ν_0 has been *formally* attributed to the $3N$th eigenfrequency of the equilibrium crystal. Electronic contributions to the entropies are neglected in equations (4) and (5). (As has been argued by Hatcher *et al* [16], electronic contributions to the formation entropy are proportional to the electronic density at the Fermi energy $n(E_F)$. The electronic contribution to the formation entropy is therefore proportional to the change of the density of states at E_F. These contributions are negligible for FCC metals because $n(E_F)$ is usually very small in FCC metals. Considerably larger values can be expected for BCC transition metals with a large density of states at the Fermi level.)

2.2. *The migration enthalpy* H_v^m

The activation energy $E_a \simeq H_v^m$ in equation (2) is the internal energy needed to move the jumping atom adiabatically from its initial to its final position. This energy consists of two parts, the change in potential energy and the change in vibrational energy. For heavy atoms, to which our calculation is restricted, the potential energy term is the dominant one and the latter term, which is of the order of 0.01 eV, can be omitted.

We assume a smooth energy curve $E(x)$ in the reactive coordinate x. For any given shape the curvature in the minimum will be related to the barrier height.

For a sine shape one has, for example,

$$E(x) = \tfrac{1}{2}E_a[1 - \cos(\pi x/d)] \tag{6}$$

where E_a is the barrier height and d the distance to the saddle point. For small deviations from the equilibrium positions at $x = 0$, equation (6) can be expanded to

$$E(x) = \tfrac{1}{2}E_a[1 - 1 + \tfrac{1}{2}(\pi/d)^2x^2] = \tfrac{1}{2}E_a(\pi^2/2d^2)x^2. \tag{7}$$

The latter equation can be expressed by harmonic lattice theory (e.g. [17]) in terms of the static lattice Green function matrix $\mathbf{G}$ of the jumping atom. If one exerts a force $\boldsymbol{F}$ on an atom m, the displacement of this atom is given by

$$\boldsymbol{s}^m = \mathbf{G}^{mm}\boldsymbol{F}^m. \tag{8}$$

All the other atoms will relax in order to minimize the elastic energy to a value of

$$E_{el} = \tfrac{1}{2}\boldsymbol{F}^m\mathbf{G}^{mm}\boldsymbol{F}^m. \tag{9}$$

Inverting equation (8) to $\boldsymbol{F}^m = (\mathbf{G}^{mm})^{-1}\boldsymbol{s}^m$ the energy can be expressed in terms of the displacement

$$E_{el} = \tfrac{1}{2}\boldsymbol{s}^m(\mathbf{G}^{mm})^{-1}\boldsymbol{s}^m. \tag{10}$$

Setting $\boldsymbol{s}^m = x\boldsymbol{e}^m$ ($x^2 = \boldsymbol{s}^m \cdot \boldsymbol{s}^m$) and comparing (7) with (10) one gets

$$E_a = (2/\pi^2)e(\mathbf{G}^{mm})^{-1}ed^2. \tag{11}$$

In deriving this equation, it has been assumed that the curvature of the effective potential is the same in the equilibrium position and in the saddle point. In general, one expects an improvement by averaging the two curvatures, i.e. replacing $\mathbf{G}^{-1}$ by the average

$$\mathbf{G}^{-1} = \tfrac{1}{2}\left(\mathbf{G}_{equ}^{-1} - \mathbf{G}_{saddle}^{-1}\right). \tag{12}$$

Here $\mathbf{G}_{\text{equ}}$ refers to a relaxed lattice around the vacancy and the jumping atom at its equilibrium position, and $\mathbf{G}_{\text{saddle}}$ refers to a lattice with the atom on the saddle point. Simulations with computer models based on various interaction potentials showed that equation (11) together with (12) reproduces the exact value of E_a within a few per cent [18].

The Green function $\mathbf{G}$ for both the equilibrium and saddle-point configurations can be expressed in terms of the eigenvalues ω^σ and eigenvectors e^σ of the dynamic matrix of the respective configuration:

$$\mathbf{G}^{mm}_{\alpha,\beta} = \frac{1}{3N}\sum_{\sigma} e^{m\sigma}_{\alpha} e^{m\sigma}_{\beta} \frac{1}{M(\omega^\sigma)^2}. \tag{13}$$

Each mode σ contributes to the Green function with the squared component of the amplitude of atom m and the Green function is inversely proportional to its square frequency. The activation energy is therefore strongly influenced by low-frequency modes. This is particularly evident in situations where the diffusing atom vibrates with low-frequency resonant modes. A long-known example for such a situation is the self-interstitial atom in FCC metals, where both low-frequency resonant vibrations and low activation energies have been observed [19, 20].

Unfortunately the Green functions needed to evaluate equations (11) and (12) are not accessible experimentally. We have therefore to resort to correlating them with their ideal crystal counterpart. For a given structure, FCC or BCC, the configurations of the vacancy and for the saddle point will be similar, whereas the vibrational spectra will differ from material to material. It is therefore a plausible assumption to absorb the structural effects in a common factor. This approximation has been checked by computer simulations with various pair potentials, and for both FCC and BCC a value of about 1.8 has been found.

In the ideal cubic lattice the Green function $\mathbf{G}^{mm}$ is diagonal and reduces to one number G^0 proportional to the ω^{-2} moment of the spectrum. It is convenient to express the distance d in units of the lattice vector a as $d = d_0 a$ and thus

$$E_a = [2/(1.8\pi^2)]\,(G^0)^{-1} d_0^2 a^2 = \alpha (G^0)^{-1} a^2 \tag{14}$$

where in the latter expression the various geometrical factors have been combined to $\alpha_{\text{FCC}} = 0.0135(7)$ and $\alpha_{\text{BCC}} = 0.0130(7)$. It should be noted that in the FCC lattice $d_0 = \frac{1}{4}\sqrt{2}$ is given by the symmetry. In the BCC lattice the corresponding value would be $d_0^{\text{sym}} = \frac{1}{6}\sqrt{3}$. In the simulations we find a value of about $d_0 = \sqrt{0.12}$, i.e. a kind of double-hump potential with relaxed positions of the barriers. The uncertainty in d_0 and in the factor 1.8 seem to correlate somewhat such that the combined uncertainty in a is reduced to about $\pm 5\%$.

In the high-temperature approximation the mean-square displacement can be expressed as

$$(u_x^2) = k_B T G^0 = 3\hbar^2 / k_B \theta_D^2 M \tag{15}$$

which explains the observed correlation between large Debye–Waller factors or small Debye temperatures θ_D and high diffusivities [21].

For practical purposes G^0 will be calculated directly from the phonon density of states $Z(\omega)$, which is known from Born–von Karman (BVK) fits to the *measured* phonon dispersions. So, instead of equation (13), the equation

$$G^0 = \int \frac{Z(\omega)}{M\omega^2}\,\mathrm{d}\omega \tag{16}$$

is used.

In the long-wavelength limit the phonon frequencies can be expressed as $\omega_j(q) = c_j(\hat{q})q$, where $c_j(\hat{q})$ is the sound velocity for polarization j and direction $\hat{q} = q/q$. If one approximates equation (16) by this long-wavelength behaviour one gets

$$G^0 = \frac{1}{3\rho}\left(\frac{3}{4\pi^4 V_c}\right)\frac{1}{3}\sum_{j=1}^{3}\left\langle\frac{1}{c_j^2}\right\rangle \tag{17}$$

where ρ is the mass density, V_c the volume of the primitive unit cell and $\langle\ \rangle$ denotes the average over all directions $\hat{q}$. These averages cannot be evaluated exactly for cubic lattices. In the isotropic case one would obtain an average of $1/c_L^2+2/c_T^2$, with c_L and c_T the longitudinal and transverse sound velocities, respectively. If for the anisotropic case one makes a crude approximation $c_L = (C_{11}/\rho)^{1/2}$, $c_{T_2} = (C_{44}/\rho)^{1/2}$ and $c_{T_1} = [(C_{11}-C_{12})/2\rho]^{1/2}$ corresponding to the sound velocities in the [110] direction expressed in terms of the elastic constants C_{ij}, one obtains an expression similar to the one used by Flynn (see below), except for the different weight of the longitudinal branch. Since $C_{11} \gg \frac{1}{2}(C_{11} - C_{12})$, this different factor is numerically of no great consequence.

The migration enthalpy derived by Flynn [22] for the continuum limit reads

$$H_v^m = C\Omega\delta^2 \tag{18}$$

with

$$\frac{15}{2C} = \frac{3}{C_{11}} + \frac{2}{C_{11}-C_{12}} + \frac{1}{C_{44}}. \tag{19}$$

Ω is the atomic volume and $\delta = q/s$ is a dimensionless constant that reflects the ratio of a hypothetical cut-off distance q of the harmonic potential towards the saddle point and the saddle-point distance s. The obvious drawback of the expressions (18) and (19) is that they limit the consideration of phonons to elastic constants. Low-energy phonons at the Brillouin zone (BZ) boundary, which are of crucial importance for the group III and IV metals [23], are taken into account only in a very indirect way by an effective lowering of C. Furthermore, equation (18) is not parameter free, no explicit values are given for the constant δ, and in practice this constant is found by adjusting equation (18) to some well known values of H_v^m.

2.3. The formation entropy S_v^f

According to equation (5) the formation entropy S_v^f can be seen as the difference of the vibrational entropies of (i) a lattice with one vacancy and an additional atom on the surface and (ii) the perfect lattice, $S_v^f = S_{vib}(\text{perfect}) - S_{vib}(\text{def})$ (see also [16]). In general $S_v^f > 0$ since a softening of the lattice is expected when an empty lattice site is introduced. This is clear from the argument that cutting of a bond that connects an atom to its neighbour leads to a reduction of the vibration frequency of the atom. The eigenmode frequencies ω_α are calculated from the force constants ϕ_{ij} known from BVK fits to the measured phonon dispersions. The enthalpy of the defect crystal has been calculated by taking one atom out of a model crystal of 432 atoms with periodic boundary conditions. The vacancy is then mimicked by the missing force constants from the empty lattice sites to all sites. No relaxation of the atoms around the vacancy have been taken into account. Tests with a relaxed crystal showed only a small decrease of S_v^f of the order of 10%. The method has been developed earlier [16, 24, 25] and, for instance, proved to be successful for calculations of α-Fe where $S_v^f = 2.1k_B/\text{atom}$ has been found.

2.4. The migration entropy S_v^m and formation enthalpy H_v^f

An equivalent simulation can be used to compute the migration entropy S_v^m. In this case an NN atom of our model crystal with a vacancy is put at the saddle-point position. In order to calculate the eigenmodes of an atom at the saddle-point position, the curvature of the potential at the saddle point has to be known precisely. Simulations with different pair potentials showed an explicit dependence of S_v^m from the chosen potential. So, the concept of a separation of structure-specific and element-specific contributions to S_v^m failed, and no direct calculation of S_v^m can be presented.

The formation enthalpy H_v^f in metals is dominated by electronic effects. Since we confine ourselves here to the contributions of the phonons to the diffusivity, no calculations of H_v^f will be presented.

3. H_v^m in FCC metals

Table 1 shows calculations of H_v^m by means of equation (14) for the best-investigated FCC metals. All phonon dispersions used to calculate the lattice Green function G^0 refer to room-temperature (RT) measurements and are reviewed in [26]. Correspondingly, lattice parameters that enter in equation (14) refer also to RT.

Table 1. Activation enthalpies for FCC metals (eV).

	H_v^m(exp) [a]	H_v^m [b]	H_v^m(Fl) [c]	H_v^f(exp) [a]	Q(exp) [d]
Ag	0.66(0.05)	0.66–0.73	0.63	1.11(0.05)	1.76
Al	0.61(0.03)	0.60	0.66	0.67(0.03)	1.25–1.31
Au	0.71(0.05)	0.74	0.64	0.93(0.04)	1.73
Cu	0.70(0.02)	0.67	0.65	1.28(0.05)	2.05
Ni	1.04(0.04)	0.98	1.11	1.79(0.05)	2.88
Pb	0.43(0.02)	0.34–0.37	0.37	0.58(0.04)	1.05–1.10
Pt	1.43(0.05)	1.26	1.41	1.35(0.05)	2.69

[a] Recommended experimental migration enthalpy H_v^m(exp) and vacancy formation enthalpy H_v^f(exp) [27].
[b] Calculated H_v^m according to equation (14).
[c] Calculated H_v^m(Fl) according to Flynn's formula (equation (18)) with $\delta^2 = 0.081$.
[d] Activation energy for self-diffusion; for curved Arrhenius plots the activation energies corresponding to the low-temperature diffusivities have been taken from [28].

The experimental values H_v^m(exp), with which our calculations have to be compared, stem from a recent review of Ehrhart [27]. Most of these values have been determined from resistivity annealing measurements around stage III after low-temperature irradiation. Therefore, these values are valid for temperatures around stage III. It is emphasized that this determination of H_v^m is independent of self-diffusion measurements; in particular H_v^m has not been chosen in order to comply with the relation $H^m + H^f = Q$.

The comparison of H_v^m with H_v^m(exp) shows excellent agreement within one standard deviation σ of the recommended experimental values. Exceptions are Pb and Pt, where the differences between recommended and calculated values are of the order of 3σ.

A similar good agreement is achieved when H_v^m(exp) is compared to calculations of H_v^m(Fl) according to Flynn's formula (equation (18)). As mentioned earlier,

equation (18) is not a parameter-free calculation of H_v^m and the constant $\delta^2 = 0.081$ has been determined such that the mean-square deviation between H_v^m(exp) and H_v^m(Fl) becomes minimum (a method applied earlier, see [19]). Because Flynn's formula relies on harmonic considerations, the elastic constants and the atomic volume have been taken at liquid-helium temperatures. For a recent compilation of elastic constants measured by ultrasound methods, we refer to [29]. According to Flynn [22] the reason for this excellent description of H_v^m is that the atoms overcome the diffusion barrier by *kinetic* energy fluctuations achieved at small displacements, i.e. near the equilibrium where the kinetic energy is the largest and the harmonic approximation is valid.

It is instructive to check to what extent H_v^m satisfies the relation $H^m + H^f = Q$. Again, the experimental values of H_v^f have been taken from [27] and are recommended averages from experiments that measure the vacancy concentration, i.e. quenched-in resistivity, positron lifetime and Simmons–Balluffi type experiments. The activation energies for self-diffusion Q stem from diffusivity measurements compiled in [28]. In cases where remarkable curvatures in the slope of the Arrhenius presentation of $D(T)$ have been reported, the compiled values of Q refer to 'low'-temperature data of $D(T)$. With the exception of Pb the relation $H_v^m + H_v^f = Q$ is obeyed well, thereby again giving evidence that self-diffusion in FCC metals is largely dominated by single vacancies.

4. H_v^m in BCC metals

Most of the BCC metals transform from a high-temperature BCC structure to a close-packed structure at low temperature or at elevated pressure. These martensitic transitions and the extreme sensitivity of BCC metals to impurities make experimental access to the migration and formation enthalpies of vacancies a difficult task. As a consequence, reliable values for H_v^m(exp) and H_v^f(exp) are only available for the group V and VI metals, where BCC is the only stable structure, and for the alkalis Li, Na and K. For BCC metals these values are compiled in a recent review by Schultz [30] and the recommended values are given in table 2. As for the FCC metals H_v^m(exp) is determined mainly by stage III resistivity annealing after low-temperature irradiation, whereas H_v^f(exp) stems from measurements of the vacancy concentration $c_v(T)$ via quenched-in resistivity, positron lifetime analysis or Simmons–Balluffi type experiments.

Reliable phonon dispersion measurements are available for a large number of BCC structures (see for instance [26]). Extensive phonon measurements have been published recently for the high-temperature BCC phase of the group IV metals Ti, Zr and Hf [9–11]. These are of particular interest because diffusion anomalies are most pronounced in these elements. Table 2 lists our calculation of H_v^m on the basis of these measured phonon dispersions. The crucial point is the correct evaluation of the static Green function G^0 by means of BVK fits to the dispersion. In cases where these BVK parameters were not available in the literature or were doubtful, the BVK fits have been repeated.

Let us first discuss those cases where the calculations of H_v^m can be compared directly with experimental values. In view of the considerable experimental uncertainties and the fact that equation (14) does not incorporate any parameter adjusted to data of diffusion experiments, the agreement between calculations and

experiment is excellent for the group V and VI metals and for α-Fe. Keeping in mind that we want to introduce temperature-dependent quantities, it is emphasized that both the experimental and the calculated migration enthalpies refer roughly to the same temperature range. The phonon dispersions were measured at RT and the resistivity stage III varies between 170 and 900 K for the group V and VI metals and α-Fe [30]. A comparison of the phonon dispersion in the alloy $Ta_{1-x}W_x$ [38] and pure Ta [41] indicates that the transverse $T_1[\xi\xi 0]$ branch in the alloyed system but extrapolated to $x = 0$ has considerably lower frequencies than determined directly in pure Ta. Therefore, the phonon measurements on pure Ta have been discarded and G^0 has been extrapolated from the $Ta_{1-x}W_x$ system to $x = 0$. The alkali metals Li, Na and K exhibit an unusually low experimental migration enthalpy $H_v^m(\text{exp})$. Whereas our calculation reproduces this tendency qualitatively, the actual values of H_v^m are a factor of 2 too large. We shall come back to this point below.

The considerable advantage of equation (14) is to make predictions where H_v^m cannot be determined experimentally, as for instance in the group III and IV metals, where the BCC phase exists only at elevated temperatures. Table 2 shows predictions for all BCC structures where phonon dispersions are known (without lanthanides and actinides). Pronounced group systematics are discernible (figure 2(*a*)). Group I metals show the lowest migration barrier, definitely below 0.1 eV. These barriers increase continuously when filling the s band and consecutively the d band up to four d electrons in group VI metals. Emphasis is put on the group III and IV transition metals, where especially low values of H_v^m are found far away from any rule of thumb predicting H_v^m only slightly smaller than H_v^f.

We finish this comparison by compiling $H_v^m(\text{Fl})$ calculated in the elastic continuum approach according to equation (18). As for the FCC metals the elastic constants and the atomic volume have been taken at liquid-helium temperature whenever possible. In cases where the BCC phase is only stable at elevated temperatures, values close to the transition temperature have been chosen. When ultrasound elastic constants were available, the figures stem from [29]. In all other cases the elastic constants have been determined from phonon measurements. In view of the uncertainty of the experimental values of $H_v^m(\text{exp})$, a different procedure than in the case of the FCC metals has been adopted to adjust the parameter δ^2. Because W is a typical representative of what we call normal self-diffusivity, $\delta^2 = 0.041$ has been adjusted in order to reproduce $H_v^m(W) = 1.7$ eV. In general $H_v^m(\text{Fl})$ coincides with our calculations of H_v^m, and in cases where $H_v^m(\text{exp})$ is known it reproduces the experimental values.

Because equation (18) represents a long-wavelength limit, we would have expected that Flynn's formula fails in those BCC metals where particularly low frequencies at large q are found [8]. However, it happens that in BCC metals the valley of transverse low-energy phonons that spans from the W to the N point is *always* connected with a low slope of the $T_1[\xi\xi 0]$ phonon branch [23]. The square of this slope determines $C' = \frac{1}{2}(C_{11} - C_{12})$, which (owing to its small value) is the dominant elastic constant in equation (19). It is due to this connection of the short-wavelength phonons with C' that Flynn's formula holds also for metals with dominant low-frequency phonons at large q.

Whereas our calculations systematically overestimate H_v^m for the three alkali metals Li, Na and K, the calculations by means of Flynn's formula reproduce the measured migration enthalpy exactly. One way to explain this could be a discrepancy in the value of the elastic constants as determined by ultrasonic measurements or by

measuring the phonon dispersion at small q. Indeed free BVK fits to Li systematically yield a C' 25% larger than measured by ultrasonics. We then forced the BVK fit to the C_{ij} values determined by the ultrasonic measurements [42], resulting in a still perfect reproduction of the measured phonons [43]. However, H_v^m only decreased by 10% with respect to the values given in table 2. We have to conclude that for the alkali metals the present *ansatz* overestimates the role of phonons at large q.

The same trend was observed in computer calculations of the activation enthalpies of Li and Na [44]. The reason for this discrepancy is probably inherent in the low values of the migration enthalpy itself. The Vineyard expression for the diffusion constant (1) assumes that the migration enthalpy is large compared with the typical phonon energies, $H^m \gg k_B\theta_D$. This condition is violated in the alkali metals, and the diffusion constant is no longer given by a product of a quasi-static activation term times an entropy factor.

For selected cases table 2 also lists the formation entropy S_v^f calculated according to the procedure described in section 2.3. As in the case of H_v^m, it is important to note that S_v^f has been calculated by means of force constants ϕ_{ij} relating to phonons measured at a given temperature. S_v^f will be discussed in more detail later on; here we confine ourselves to the statement that S_v^f is of the order of magnitude generally expected for the formation entropy.

5. Temperature-dependent $H_v^m(T)$

Our approach to calculate H_v^m and S_v^f has the advantage of relying on realistic interactions at a given temperature. Anharmonicities of the lattice potentials, which manifest themselves as shifts of the phonon frequencies with temperature, are taken into account in a quasi-harmonic approach. Calculating H_v^m or S_v^f by means of phonon dispersions measured at different temperatures automatically introduces the temperature dependence of these quantities.

Confining ourselves to BCC metals, one is confronted with the problem that only for a few cases has the whole phonon dispersion been measured at different temperatures. Furthermore *all* these examples refer to temperatures below the temperature where diffusion constants $D(T)$ can be measured! That is why we started a series of experiments measuring phonon dispersions for the first time in a temperature range relevant for tracer diffusion coefficients. For that purpose we selected the two extreme cases β-Zr and Cr; the temperature-dependent dispersion of β-Zr has been published recently [10] and those of Cr are the topic of a forthcoming paper [45].

Table 3 compiles the values of H_v^m and S_v^f calculated from the available phonon dispersion for β-Zr and Cr at different temperatures. For completeness, calculations for Nb and Mo, where phonons are known over a large temperature range, are added.

For β-Zr the transverse low-energy phonons along $T_1[\xi\xi 2\xi]$ and $T_1[\xi\xi 0]$ are partly overdamped. Consequently they have been described by a damped oscillator equation, yielding a large phonon width or a short phonon lifetime and a phonon energy that is higher than the energy where the highest count rate is observed [10]. Similar to temperature-dependent energy shifts, this very short lifetime of the phonon (in the order of vibrational periods) is a signature of strong anharmonicity. Taking the phonon energy from a damped oscillator description of the phonon groups in order to calculate $Z(\omega)$ and consecutively G^0, this part of the anharmonicity is neglected.

Table 2. Activation enthalpies for BCC metals (eV).

	H_v^m(exp) [a]	H_v^m [b]	H_v^m(Fl) [c]	H_v^f(exp) [a]	$S_v^f(k_B/\text{atom})$ [d]	Q_1 [e]	Q [f]
Li	0.038	0.073 (110 K)	0.035 (80 K)	0.48		0.55	0.57
Na	0.03	0.076 (90 K)	0.039 (75 K)	0.34		0.37	0.44
K	0.038	0.070 (9 K)	0.037 (0 K)	0.34		0.39	0.41
Rb		0.056 (120 K)[g]	0.038 (120 K)				0.41
Cs		0.048 (RT)[h]	0.038 (RT)				
β-Ca		0.19 (726 K)[i]	0.10 (726 K)				
γ-Sr		0.15 (930 K)[j]	0.11 (930 K)				
Ba		0.24 (RT)[k]	0.17 (RT)				
β-Sc		0.29 (1673 K)[l]	0.22 (1673 K)				
γ-La		0.15 (1143 K)[m]	0.06 (1143 K)				1.2
β-Ti		0.31 (1293 K)[n]	0.22 (1293 K)		2.4 (1293 K)		
β-Zr		0.28 (1188 K)[o]	0.21 (1188 K)		2.8 (1188 K)		
β-Hf		0.39 (2073 K)[p]	0.39 (2073 K)		2.5 (2073 K)		
V	0.5	0.47 (RT)	0.51 (4 K)	2.1		2.9[r]	3.2
Nb	0.55	0.54 (RT)	0.56 (4 K)	2.7		3.7[r]	4.1
Ta	0.7	0.70 (RT)[q]	0.84 (4 K)	3.1		3.8[r]	4.4
Cr	0.95	0.88 (RT)	0.96 (4 K)	2.1/2.7[v]	1.8 (RT)	4.2[s]	4.58[s]
Mo	1.35	1.22 (RT)	1.38 (4 K)	3.2	1.8 (RT)	4.5[t]	5.0
W	1.7	1.62 (RT)	1.70 (4 K)	3.6		5.4[r]	6.5
α-Fe	0.55	0.66 (RT)	0.57 (4 K)	1.8	2.1	2.95–2.57[u]	

[a] Recommended experimental migration enthalpy H_v^m(exp) and vacancy formation enthalpy H_v^f from [30].
[b] Calculated H_v^m according to equation (14); note the temperature for which H_v^m has been calculated.
[c] Calculated H_v^m(Fl) according to Flynn's equation (18) with $\delta^2 = 0.041$.
[d] Calculated formation entropy S_v^f according to equation (5).
[e] Activation enthalpy Q_1 for self-diffusion at $T \sim \frac{1}{2}T_m$.
[f] Activation enthalpy Q for a straight-line fit to the Arrhenius plot of $D(T)$ over the whole measured temperature range.
Sources: Phonon energies and elastic constants to calculate H_v^m and S_v^f stem from [26] and [29] or from: [g] [31], [h] [32], [i] [33], [j] [34], [k] [35], [l] [36], [m] [37], [n] [9], [o] [10], [p] [11], [q] extrapolated from $Ta_{1-x}W_x$ [38], Q_1 or Q stem from [28] or from: [r] [3], [s] [4], [t] [39], [u] [40].

Lacking a proper way to take the damping into account in $Z(\omega)$, we adopted an alternative approach: the damped phonons were described by broadened Gaussians, yielding phonon energies that correspond to the energy of highest count rate in the phonon groups [46]. The phonon energies thus determined are of even lower energy than that from the damped oscillator description. Owing to the dominance of the low-energy phonons in the determination of G^0, this alternative procedure leads to lower migration enthalpies H_v^m. The results of both procedures are listed for the case of β-Zr in table 3. For all other metals of table 3, phonons are not particularly damped and both descriptions of the phonons lead to identical phonon energies and therefore identical values of H_v^m.

Table 3. Variation of H_v^m and S_v^f with temperature directly calculated from the phonon dispersion at the respective temperature.

	T (K)	H_v^m (eV)	$S_v^f(k_B)$
BCC Zr[c]	1188	0.284[a] (0.257)[b]	2.76[a] (3.32)[b]
	1483	0.324 (0.308)	2.58 (2.84)
	1883	0.374 (0.337)	2.38 (2.66)
Nb[d]	298	0.54	
	700	0.59	
	900	0.63	
	1030	0.64	
Cr[e]	298	0.88	1.8
	673	0.85	1.8
	1073	0.77	1.8
	1473	0.69	1.8
	1773	0.59	1.9
Mo[f]	10	1.26	1.8
	298	1.22	1.8
	1203	1.09	1.8

[a] Based on a description of the low-energy phonons by a damped oscillator.
[b] By a Gaussian lineshape.
Sources: References for the phonon dispersions are: [c] [10, 46], [d] [47], [e] [45], [f] [48].

Figure 2(*b*) gives an impression of the temperature dependence of $H_v^m(T)$ for β-Zr and Cr. In both cases $H_v^m(T)$ can be interpolated by a curved polynomial. Taking into account the uncertainties in determining H_v^m, this curvature is not conclusive; a linear extrapolation is also compatible with the data. What is of particular importance here is the opposite temperature dependences of $H_v^m(T)$ in these metals. Because phonons stiffen with increasing temperature in β-Zr, H_v^m increases; and because in Cr the opposite happens, there $H_v^m(T)$ decreases with increasing temperature.

6. Comparison with tracer diffusivities

The unknown attempt frequency $\nu = \nu_0 \exp(S_v^m/k_B)$ and the experimentally less well known H_v^f do not allow a direct calculation of $D(T)$. However, using the values of table 3, ν and H_v^f can be estimated by a fit of equation (1) to the known tracer diffusivities.

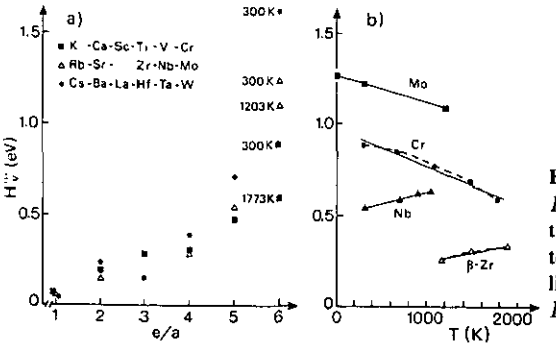

Figure 2. (*a*) The e/a systematics of the calculated H_v^m for BCC metals. For the group VI metals the increase of H_v^m is less pronounced at high temperatures. The corresponding temperatures are listed in table 2. (*b*) Temperature dependence of H_v^m for selected BCC metals.

6.1. β-Zr

Figure 3 shows such a comparison or compatibility check for β-Zr based on either a Gaussian or a damped oscillator description of the phonons. From the comparison of calculated and measured $D(T)$ and assuming as a first approximation constant values of ν and H_v^f, one finds the following:

(i) $\nu = 1.8 \times 10^{11}$ Hz or 1.9×10^{11} Hz, which agrees with our expectations of ν being of the order of typical phonon frequencies.

(ii) $H_v^f = 1.28$ eV or 1.35 eV, which compares favourably with the calculations of Willaime and Massobrio [49], who find $H_v^f = 1.53$ eV. Experimental values of H_v^f are not available [50].

(iii) Using a Gaussian description of the phonon frequencies, the curvature of the Arrhenius plot is reproduced.

The latter statement is only qualitative. Uncertainties in the calculations of H_v^m are too large to make any definite conclusion on a non-linear temperature dependence. Only a non-linear temperature dependence creates a curvature in an Arrhenius plot. It is emphasized that it is not the reproduction of the curvature that is the crucial point for temperature-dependent diffusion quantities, but rather it is the explanation of the relatively high diffusivity in β-Zr at low temperature.

6.2. Cr

Figure 4 shows the corresponding plot for Cr. As mentioned before, Cr shows the inverse temperature dependence of the phonon energies as compared to β-Zr. Within our model this means a relatively high diffusion barrier at low temperature, which decreases with increasing temperature. Obviously this corresponds to the experimental observation that diffusivities are particularly low at low temperatures.

The peculiarity of Cr, namely the reproduction of the Arrhenius plot of $D(T)$ by a single activation energy $Q = 4.58$ eV over a temperature range from $\frac{1}{2}T_m$ to T_m, then necessarily demands a temperature-dependent $H_v^f(T)$. Using the values of table 3 and assuming a fixed attempt frequency $\nu = 10^{12}$ Hz, $D(T)$ can be reproduced with $H_v^f(T) = 2.77$ eV at 1073 K decreasing to 2.01 eV at 1773 K. For Cr, H_v^f has been determined independently by positron lifetime measurements [51]. Close to the melting point an average value of $H_v^f(T) = 2.1 \pm 0.3$ eV is found. As has been shown for measurements in the group IV metals [50], this method exhibits large systematic errors for some refractory metals and the experimental value may be too low. Recent *ab initio* calculations of H_v^f based on the multiple scattering

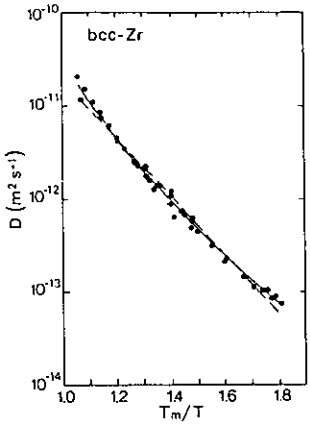

Figure 3. $D(T)$ for BCC Zr: data points from [49]; full curve and broken line, reproduction of $D(T)$ based on either a Gaussian or a damped oscillator description of the phonons in β-Zr (for details, see text).

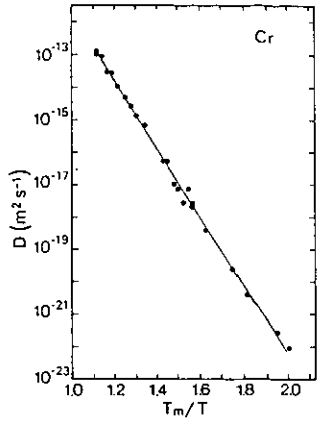

Figure 4. $D(T)$ for Cr: data points from [4]; full line, reproduction of $D(T)$ by means of temperature-dependent migration and formation enthalpies (for details, see text).

approximation of Korringa, Kohn and Rostoker (KKR method) indicate an upper limit for $H_v^f = 2.7$ eV in Cr [52] in agreement with our estimation at $\frac{1}{2}T_m$.

6.3. Limitations

The above estimates of ν and H_v^f yield values of the expected order of magnitude. They should by no means be understood as quantitative. For instance, equation (4) and our knowledge of the strong anharmonicity of the phonons in β-Zr as well as in Cr strongly suggest a temperature-dependent migration entropy $S_v^m(T)$ and thereby an attempt frequency changing with temperature. The observed shifts of the phonon frequencies with temperature reveal that the effective potential in which the atoms vibrate changes with temperature. It is therefore plausible that the formation enthalpy H_v^f needed to form vacancies also changes with temperature.

This conclusion, that *all* quantities determining $D(T)$ depend explicitly on temperature, is further supported by thermodynamic considerations. It is well known that

$$(\partial H/\partial T)|_p = T(\partial S/\partial T)|_p \tag{20}$$

holds with H and S the activation enthalpy and the entropy of the diffusion process. Making use of equations (1) and (20), it can easily be shown that the slope of the diffusivity in the Arrhenius plot

$$\partial \ln D(T)/\partial(1/k_B T) = H(T) \equiv Q(T) \tag{21}$$

gives at any point the temperature-dependent activation energy $Q(T)$ of the diffusion process [54].

Assuming that the formation and migration of the vacancy are independent thermodynamic quantities—the implicit assumption of the validity of equation (1)—$H(T)$ decomposes into

$$H(T) = H_v^f(T) + H_v^m(T) \tag{22}$$

and equation (20) is also valid separately for H^i and S^i with the indices $i = m, f$. The temperature dependence of $H_v^m(T)$ then determines the temperature variation of the migration entropy $DS_v^m(T)$, and an $S_v^f(T)$ decreasing with temperature as found for β-Zr necessarily needs a decreasing $H_v^f(T)$. It is evident that, if $H_v^m(T)$ and $S_v^f(T)$ change with temperature as shown in table 3, the quantities $H_v^f(T)$ and $S_v^m(T)$ do so, too.

Contradictions of our calculations in section 5 to these general thermodynamic considerations have to be mentioned. $H_v^m(T)$ increases for the case of β-Zr with increasing temperature. Together with the measured change in $Q(T)$ from 1.10 eV at 1188 K to 1.67 eV at 1883 K, this leads according to equation (22) to a $H_v^f(T)$ increasing with temperature. If equation (20) is also valid for the formation process alone, then $\partial S_v^f/\partial T$ has to be positive, whereas our microscopic calculations of $S_v^f(T)$ show the opposite trend. One should note, however, that at $T = 1883$ K $\exp[-H_v^m(T)/k_B T] \simeq 0$, and, therefore, the condition of well separated single atom jumps with full thermalization in between is no longer fulfilled. This was also observed in a computer simulation by Willaime and Massobrio [55] (see below).

7. Other approaches to calculate H_v^m

Using a Chang–Graham potential and both the Green function and energy minimization methods, Hatcher *et al* [16] calculated the diffusion properties of α-Fe. A formation enthalpy $S_v^f = 2.1k_B$ and an attempt frequency $\nu = 3.4 \times 10^{13}$ Hz are found, whereby S_v^f is in astonishingly good agreement with our calculations. Diffusion is by hopping over a double-hump potential with the first hump at a relaxed position of $0.338a$ instead of $\frac{1}{6}\sqrt{3}a$.

Using a Finnis–Sinclair interatomic potential for α-Fe, Marchese *et al* [56] also find a relaxed double-hump potential for the migrating defect with a small minimum between the double humps of only 0.02 eV. With such a potential they got values of $H_v^m = 0.92$ eV and $H_v^f = 2.26$ eV.

Using a Dagen's type of pair potential, static calculations by Schober *et al* [44] yield $H_v^m = 0.11$ eV in Li. Dynamical simulations with the same potential by Da Fano and Jacucci [57] for Na and K give migration enthalpies in the range of 0.09–0.18 eV. Compared with the experimental values [58] and the present calculation, all these figures in the alkali metals are definitely too high.

Detailed simulations of diffusion properties for the case of β-Zr have been performed by Willaime and Massobrio [49]. By means of quenched molecular dynamics, the diffusion trajectory of a migrating atom is followed; 99% of all atomic jumps turned out to be NN jumps. At 0 K and the lattice fully relaxed, values of $H_v^m = 0.32$ eV, $H_v^f = 1.53$ eV and $S_v^f = 0.5k_B$ are found. Increasing the temperature, the effective migration barrier decreases and $H_v^m = 0.284$ and $\nu = 7.1 \times 10^{12}$ Hz are found. In contrast to the simulations in α-Fe the migration barrier relaxes to a single peak in the dynamic case as well as in the static case (0 K). Relevant for the diffusion anomalies in BCC metals is a further observation made in the course of these molecular dynamic simulations. At ~ 1600 °C the time interval between two successive jumps of the vacancy is approximately equal to the duration of an atomic jump from one site to the nearest-neighbour site. This means that when an atom finishes its jump into the vacancy the next diffusing atom has already started to jump. In this context it might be necessary to reconsider the assumption of neglecting the migration events

in order to calculate the vacancy concentration, i.e. the formation and migration can no longer be considered as thermodynamically independent processes. This might be one of the reasons why the thermodynamic considerations partly contradict the calculated temperature dependence of S_v^f in the case of β-Zr.

Temperature-dependent activation enthalpies $H(T)$ and $S(T)$ have also been proposed by Gilder and Lazarus [59] and in a more explicit way by Varotsos and Alexopoulos [54]. The bulk quantities to probe the lattice anharmonicities are the thermal expansion coefficients and the bulk modulus $B = (C_{11} + 2C_{12})/3$. Complementary to our approach, these studies concentrate on the temperature dependence of the activation process and the vacancy formation process. Microscopic details, as for instance the low restoring forces for the motion of the [111] chains in most BCC metals, do not enter directly in these considerations—thermal expansion and the bulk modulus are isotropic quantities in cubic metals. Whereas these models explain the observed curvature in the Arrhenius plot of $D(T)$ in BCC metals mainly by the anomalous decreases of the bulk modulus at *high* temperature, the present model explains 'unusually' high or low diffusivities at *low* temperature in accordance with the experimental observations [1, 2].

8. Summary

A model based on the static Green function has been presented to calculate the migration enthalpy H_v^m for a nearest-neighbour vacancy jump mechanism. The excellent agreement of the calculated values of H_v^m with the best-known experimental cases, namely H_v^m measured in FCC metals, shows the reliability of the method. Calculations for BCC structures, where the experimental values are less well known, allow predictions for all BCC metals where the phonon dispersions have been measured. The particularity of the open BCC structure—namely low restoring forces for the transverse motion of [111] chains and of the (110) planes against each other [23]—is implicitly taken into account. This leads to pronounced chemical group systematics in the computed H_v^m with especially low H_v^m for all the BCC elements with martensitic transformations to close-packed structures.

In quasi-harmonic approximations and by means of the measured shifts in the phonon dispersion, the temperature dependence of H_v^m is introduced. In β-Zr, where $D(T)$ is relatively high at low temperatures, the migration barrier indeed decreases when the transition temperature is approached from above. In Cr, where the diffusivity is particularly low at low temperatures, an increase of the migration barrier towards low temperatures is calculated.

Whereas mainly arguments for a temperature-dependent H_v^m have been presented, the observed pronounced anharmonicity in the lattice vibrations in such different cases as β-Zr and Cr makes it likely that the vacancy formation H_v^f also depends on temperature [54]. For β-Zr and Cr, $D(T)$ has been reproduced with a set of temperature-dependent values of H_v^m and H_v^f in the framework of a single vacancy mechanism.

In summary, we emphasize that the above calculations support the model of phonon-controlled self-diffusion in BCC metals [2, 8], where the term 'controlled' should be understood in the sense that the dynamic response of the lattice tells us about particularly low and temperature-dependent migration barriers.

The present calculations of H_v^m strongly support the model of the dominant role of monovacancy diffusion in the low- as well as in the high-temperature region

of BCC metals, but do not prove it. Experiments that measure the diffusion mechanism directly like incoherent quasi-elastic neutron scattering (QNS) are much more conclusive. Such measurements have been performed close to the melting point in Na [12, 13] and Ti [14], and clearly reveal the dominant role of NN vacancy jumps and allow at most $\sim 15\%$ of next NN vacancy jumps, possibly via divacancies. Significant interstitial contributions could not be detected. Such a mechanism is still under consideration to explain $D(T)$ in Cr near the melting point [3]. A QNS experiment in Cr should be able to clarify the situation.

Acknowledgments

Two of us (WP and JT) want to thank Ch Herzig and G Vogl for fruitful collaboration and discussions, which partly stimulated the present work. Stimulating discussions with F Willaime are gratefully acknowledged. Part of this work has been funded by the German Bundesministerium für Forschung und Technologie under contract No 03-HE2MUE-0.

References

[1] Peterson N L 1978 *Comments Solid State Phys.* **8** 93
[2] Herzig C 1983 *Diffusion in Metals and Alloys, DIMETA-82* ed F J Kedves and D L Beke (Switzerland: Trans. Tech.) p 23
[3] Siegel R W 1982 *Proc. Yamada Conf. on Point Defects and Defect Interactions in Metals* ed J Takamura, M Doyama and M Kiritani (Tokyo: University of Tokyo Press) p 533
[4] Mundy J N, Hoff H A, Pelleg J, Rothman S J, Nowicki L J and Schmidt F A 1981 *Phys. Rev.* B **24** 658
[5] Peterson N L 1978 *J. Nucl. Mater.* **69 & 70** 3
[6] Köhler U and Herzig C 1988 *Phil. Mag.* A **58** 769
[7] Petry W, Heiming A, Trampenau J and Vogl G 1989 *DIMETA-88, Defect Diffus. Forum* **66–69** 157
[8] Petry W, Heiming A, Herzig C and Trampenau J 1991 *Defect Diffus. Forum* **75** 211
[9] Petry W, Heiming A, Trampenau J, Alba M, Herzig C, Schober H R and Vogl G 1991 *Phys. Rev.* B **43** 10933
[10] Heiming A, Petry W, Trampenau J, Alba M, Herzig C, Schober H R and Vogl G 1991 *Phys. Rev.* B **43** 10948
[11] Trampenau J, Heiming A, Petry W, Alba M, Herzig C, Miekeley W and Schober H R 1991 *Phys. Rev.* B **43** 10963
[12] Ait Salem M, Springer T, Heidemann A and Alefeld B 1979 *Phil. Mag.* A **39** 797
[13] Göltz G, Heidemann A, Mehrer H, Seeger A and Wolf D 1980 *Phil. Mag.* A **41** 723
[14] Vogl G, Petry W, Flottmann Th and Heiming A 1989 *Phys. Rev.* B **39** 5025
[15] Vineyard G H 1957 *J. Phys. Chem. Solids* **3** 121
[16] Hatcher R D, Zeller R and Dederichs P H 1979 *Phys. Rev.* B **19** 5083
[17] Leibfried G and Breuer N 1978 *Point Defects in Metals I (Springer Tracts in Modern Physics 81)* ed G Höhler (Berlin: Springer)
[18] Schober H R 1987 *Physics of Phonons (Lecture Notes in Physics 285)* ed T Paszkiewicz (Berlin: Springer) p 188
[19] Ehrhart P, Robrock K H and Schober H R 1986 *Physics of Radiation Effects in Crystals* ed R H Johnson and A N Orlov (Amsterdam: Elsevier)
[20] Urban R, Ehrhart P, Schilling W, Schober H R and Lanter H-J 1987 *Phys. Status Solidi* b **144** 287
[21] Tewary V K 1973 *J. Phys. F: Met. Phys.* **3** 704
Klotsman S M 1983 *Phys. Met. Metall.* **55** 82
[22] Flynn C P 1968 *Phys. Rev.* **171** 682
[23] Petry W 1991 *Phase Transitions* **31** 119
[24] Harding J H and Stoneham A M 1981 *Phil. Mag.* B **43** 705

[25] Bechthold P S, Kettler U, Schober H R and Krasser W 1986 *Z. Phys.* D **3** 263
[26] Schober H R and Dederichs P H 1987 *Landolt-Börnstein* New Series, Group III, vol 13a, ed K H Hellwege and J L Olsen (Berlin: Springer) p 188
[27] Ehrhart P 1991 *Landolt-Börnstein* New Series, Group III, vol 25, ed H Ullmaier (Berlin: Springer)
[28] Mehrer H, Stolica N and Stolwijk N A 1990 *Landolt-Börnstein* New Series, Group III, vol 26, ed H Mehrer (Berlin: Springer)
[29] Hearmon R F S 1979 *Landolt-Börnstein* New Series, Group III, vol 11, ed K N Hellwege (Berlin: Springer); 1984 *Landolt-Börnstein* New Series, Group III, vol 18, ed K N Hellwege (Berlin: Springer)
[30] Schultz H 1991 *Landolt-Börnstein* New Series, Group III, vol 25, ed H Ullmaier (Berlin: Springer)
[31] Copley J R D and Brockhouse B N 1973 *Can. J. Phys.* **51** 657
[32] Mizuki J and Stassis C 1986 *Phys. Rev.* B **34** 5890
[33] Heiroth M, Buchenau U, Schober H R and Evers J 1986 *Phys. Rev.* B **34** 6681
[34] Mizuki J and Stassis C 1985 *Phys. Rev.* B **32** 8372; 1987 *Phys. Rev.* B **35** 872 (errata)
[35] Mizuki J, Chen Y, Ho K-M and Stassis C 1985 *Phys. Rev.* B **32** 666
[36] Petry W, Trampenau J and Herzig C 1993 to be published
[37] Güthoff F, Petry W, Stassis C, Herzig C, Heiming A, Hennion B and Trampenau J 1993 to be published
[38] Higuera B J, Brotzen F R, Smith H G and Wakabayashi N 1985 *Phys. Rev.* B **31** 730
[39] Maier K, Mehrer H and Rein G 1979 *Z. Metallkd.* **70** 271
[40] Lübbehusen M and Mehrer H 1990 *Acta Metall. Mater.* **38** 283
[41] Woods A D B 1964 *Phys. Rev.* **136** A781
[42] Felice R A, Trivisonno J and Schulte D E 1977 *Phys. Rev.* B **16** 5173
[43] Beg M M and Nielsen M 1976 *Phys. Rev.* B **14** 4266
Smith H G, Dolling G, Nicklow R M, Vijayaraghavan P R and Wilkinson M K 1968 *Inelastic Neutron Scattering* (Vienna: IAEA) vol 1, p 149
[44] Schober H R, Taylor R, Norgett M J and Stoneham A M 1975 *J. Phys. F: Met. Phys.* **5** 637
[45] Trampenau J, Petry W and Herzig C 1993 to be published
[46] Heiming A, Petry W, Trampenau J, Alba M, Herzig C and Vogl G 1989 *Phys. Rev.* B **40** 11425
[47] Hui J C K and Allen P B 1975 *J. Phys. C: Solid State Phys.* **8** 2923
[48] Zarestky J, Stassis C, Harmon B N, Ho K-M and Fu C L 1983 *Phys. Rev.* B **28** 697
[49] Willaime F and Massobrio C 1991 *Phys. Rev.* B **43** 11653
[50] Hood G M, Schulz R J and Carpenter G J C 1976 *Phys. Rev.* B **14** 1503
Hood G M and Schulz R J 1977 *J. Nucl. Mater.* **67** 207
[51] Campbell J L and Schulte C W 1979 *Appl. Phys.* **19** 149
Loper G D, Smedskaer L C, Chason M K and Siegel R W 1985 *Positron Annihilation* ed P C Jaim, R M Singru and K P Gopinathan (Singapore: World Scientific) p 461
[52] Drittler H B 1991 *Jül-Report* 2445
[53] Kidson G V and McGam J 1961 *Can. J. Phys.* **39** 1146
Federov J I and Lundy J S 1963 *Trans. Metall. Soc. AIME* **227** 592
Herzig C and Eckseler H 1979 *Z. Metallkd.* **70** 215
[54] Varotsos P A and Alexopoulos K D 1986 *Thermodynamics of Point Defects and Their Relaxation with Bulk Properties (Defects in Solids 14)* ed S Amelinckx, R Gevers and J Nihoul (Amsterdam: North-Holland)
[55] Willaime F and Massobrio C 1993 *Defects in Materials, MRS Symp. Proc.* ed P D Bristowe, J E Epperson, J E Griffith and Z Liliental-Weber to be published
[56] Marchese M, Zacucci G and Flynn C P 1988 *Phil. Mag. Lett.* **57** 25
[57] Da Fano A and Jacucci G 1977 *Phys. Rev. Lett.* **39** 950
[58] Wallner G 1983 *PhD Thesis* Technical University, München
Wallner G, Bönig K and Dedek U 1986 *J. Phys. F: Met. Phys.* **16** 257
[59] Gilder H M and Lazarus D 1975 *Phys. Rev.* B **11** 4916